HHS Public Access

Author manuscript

Methods Mol Biol. Author manuscript; available in PMC 2020 July 23.

Published in final edited form as:

Methods Mol Biol. 2020 ; 2101: 39–51. doi:10.1007/978-1-0716-0219-5_4.

Cover Page: In vitro microtubule dynamics assays using darkfield microscopy

Jeffrey O. Spector,

Cell Biology and Biophysics Unit, Porter Neuroscience Research Center, National Institute of Neurological Disorders and Stroke, Bethesda, MD 20892, U.S.A.

Annapurna Vemu,

Cell Biology and Biophysics Unit, Porter Neuroscience Research Center, National Institute of Neurological Disorders and Stroke, Bethesda, MD 20892, U.S.A.

Antonina Roll-Mecak

Cell Biology and Biophysics Unit, Porter Neuroscience Research Center, National Institute of Neurological Disorders and Stroke, Bethesda, MD 20892, U.S.A.

Biochemistry & Biophysics Center, National Heart, Lung and Blood Institute, Bethesda, MD 20892, U.S.A.

Abstract

Microtubules are dynamic non-covalent mesoscopic polymers. Their dynamic behavior is essential for cell biological processes ranging from intracellular transport to cell division and neurogenesis. Fluorescence microscopy has been the method of choice for monitoring microtubule dynamics in the last two decades. However, fluorescent microtubules are prone to photodamage that alters their dynamics and the fluorescent label itself can affect microtubule properties. Darkfield imaging is a label-free technique that can generate high signal-to-noise, low background images of microtubules at high acquisition rates without the photobleaching inherent to fluorescence microscopy. Here we describe how to set up and image *in vitro* microtubule dynamics using darkfield microscopy. The ability to image microtubules label-free allows the investigation of the dynamic properties of non-abundant tubulin species where fluorescent labeling is not feasible, free from the confounding effects arising from the addition of fluorescent labels.

Keywords

Microtubule dynamics; darkfield; label-free; microscopy; tubulin; microtubule

1. Introduction

Microtubules are non-covalent hollow cylindrical polymers with an outer diameter of 25nm. They are built through the addition of tubulin α-heterodimers at their tips. The first visualization of individual microtubules was achieved with darkfield microscopy in 1975 by

Correspondence: Antonina@mail.nih.gov.

Kuriyama and Miki-Noumura (1). Microtubules oscillate stochastically between growing and shrinking states. The cycle of growth, shrinkage and the rapid transition between growth and depolymerization (catastrophe) and depolymerization and growth (rescue) is known as dynamic instability (2). Dynamic instability was directly confirmed using differential interference contrast (DIC) or Nomarski microscopy (3) and darkfield microscopy (4, 5). This dynamic behavior is important for basic biological processes ranging from intracellular transport to cell division and differentiation and is highly regulated in cells by a large number of cellular effectors (6).

In vitro microtubule dynamics assays have been an essential tool for understanding the mechanism of microtubule regulators. Fluorescence microscopy, in particular total internal reflection microscopy (TIRFM), has been the dominant imaging technique for microtubules in the last two decades. This dominance over other techniques is in part due to the ease of fluorescence imaging, the low signal-to-noise ratio of DIC microscopy and the challenge in obtaining high-quality images using darkfield microscopy. Most importantly, multiplexing fluorescent microtubules with other fluorescently labeled motors and microtubule associated proteins (MAPs) allows the examination of microtubule-effector interactions in real time. However, there are several drawbacks to fluorescence-based microtubule dynamics assays: 1) The presence of the fluorophore can perturb microtubule dynamics. 2) Fluorescent tubulin photobleaches and it has been shown that photodamaged microtubules display lattice defects (7, 8) and will even break (7, 9). 3) Fluorescence imaging relies on the emission of photons from an excited molecule. Thus, image acquisition speed is limited by the number of photons emitted and collected per frame. This limits the accuracy of determining depolymerization rates, which are ~ ten-fold faster than polymerization rates. 4) Fluorescent labeling requires large tubulin concentrations as the process is inefficient. This is not easily achieved with tubulin from less abundant sources such as tubulin isolated from various cell lines (10, 11) recombinant tubulin (12, 13, 14, 15) as well as tubulin from various species such as *C. elegans* and *X. laevis* (10, 16). As a result, most fluorescently labeled tubulin used in microtubule dynamics assays is brain tubulin because of its abundance and ease of purification (17). However, tubulin isolated from brain tissue is a highly heterogeneous mixture of tubulin isoforms and posttranslational modifications (11, 12) and thus not well-suited for understanding how various tubulin isoforms or tubulin modifications affect intrinsic polymer properties and interactions with MAPs.

Recent years have seen a resurgence in label-free imaging of microtubules (12, 16, 18, 19, 20, 21, 22, 23, 24). Label-free techniques rely on imaging the light scattered by the imaged object and thus are very powerful for imaging microtubules because they contain enough mass in a diffraction-limited spot. One main advantage is that scattering techniques are not prone to photobleaching. However, this advantage can also constitute their downside since their use requires very clean surfaces and samples since stray light due to misalignment or scattered by even small amounts of aggregates will overwhelm the microtubule signal. Second, because scattered light is measured, as opposed to emitted photons, scattering techniques are only limited by the speed of the camera and the amount of light hitting the sample. Therefore, the development of high intensity LED light sources and lasers have made it possible to image microtubules label-free at high frame rates (12, 18, 21, 23).

Darkfield microscopy images the sample at an oblique angle and collects only the light that is scattered by the sample. Unlike interference reflection microscopy (IRM) and interferometric scattering microscopy (iSCAT), darkfield microscopy is not strictly limited to near-surface imaging and the microtubule contrast is generally more uniform than in interference techniques where a small distance from the surface can lead to contrast inversion. (22). Individual microtubules can be easily visualized with exposure times of 20 ms and even as low as 1 ms. A typical darkfield image of unlabeled microtubules growing from seeds immobilized to the microscope cover slide is shown in Figure 1. Darkfield imaging can be performed either though the condenser or through the objective in a total internal reflection configuration (25). The ability to image single dynamic microtubules at high frame rates, and without the complication of exogenous fluorescent molecules makes darkfield microscopy a powerful technique for imaging *in vitro* microtubules dynamics. In addition, many commercial options are readily available and easy to integrate into existing microscopes, and thus do not require custom addition of optical elements as some of the interference techniques do. The goal of this chapter is to describe how to image *in vitro* reconstituted microtubule dynamics using darkfield microscopy.

2. Materials and Equipment

2.1 Darkfield Microscopy

1. High numerical aperture (NA) (>1.4) oil immersion dark field condenser (see Note 1).
2. Adjustable NA (1.0–1.3) 100x objective lens.
3. Low magnification low NA (0.45) objective.
4. High power LED Light source.
5. sCMOS camera (For example in our lab we use a Hamamatsu Flash 4.0 v2 but there are many options available will work (Andor Zyla,Photometrics Prime 95B, PCO pco.edge).
6. Inverted microscope with objective heater (For example in our lab we use a Nikon Ti-E 2000 with perfect focus and an objective heater from Bioptechs).
7. Control Software (For example in our lab we use micromanager(27)).

2.2 Flow-Chamber Construction

1. Double-sided permanent tape (3M #34-87160599-3).
2. 22×40 mm # 1.5 coverslip cleaned and silanized as described previously(26).
3. 3”x1” x 1mm thick microscope slide cleaned and silanized as described previously(27).

2.3 Buffers and Solutions

Prepare all buffer solutions with ultrapure water (> 18 MΩ cm at 25°C) and filter using 0.22 μm bottle-top filters.

1. BRB80: 80 mM PIPES, 1mM $MgCl_2$ and 1mM EGTA (pH 6.8 adjusted with KOH).
2. GMPCPP (Jena Biosciences #NU-405S).
3. BB buffer : BRB80 supplemented with 0.1% β−mercaptoethanol.
4. BBC buffer : BB containing a final concentration of 2mg/ml casein.
5. BBP buffer : BB containing a final concentration of 0.1% Pluronic F-127 (Cat #P6866).
6. Salt Buffer (SB): BB supplemented with GTP (1mM final concentration) and KCl (100mM final concentration).
7. Neutravidin solution: 0.1mg/ml Neutravidin (see Note 2).
8. Oxygen scavengers (catalase, glucose oxidase, and 2M glucose) prepared as described previously.(27)
9. Tubulin: unlabeled tubulin purified from porcine brain (Cytoskeleton Inc.#T238P) for dynamic extensions (see Note 3) and biotin-tubulin (Cytoskeleton Inc.#T333P) for microtubule seeds.
10. GMPCPP-stabilized biotinylated microtubule seeds (see Section 3.2).
11. Dynamics buffer: tubulin at the desired concentration in BRB0 supplemented with 100 mM KCl, 1mM GTP and 0.1% pluronic F-127, 20 mM glucose, glucose oxidase, and catalase. (see Note 4).

3. Methods

3.1 Darkfield setup and alignment on an inverted microscope

1. Before beginning darkfield alignment, first set up the microscope for Köhler illumination.
2. Once Köhler illumination is achieved, insert the darkfield condenser and switch to a low-power objective (we use a 10× 0.45 NA objective for this).
3. Swab the inside of your cheek with a pipette tip and place it on a coverslip. Press the coverslip down and seal the chamber edges. Cheek cells are barely visible in transmission but are very pronounced in darkfield.
4. Place the sample on the microscope stage (coverslip down) and place a drop of immersion oil on the condenser side of the slide. Slowly bring the condenser into oil contact with the top of the slide (see Note 5).
5. Slowly focus the microscope using the focus knobs to obtain an image of the cheek cells.
6. The use of low magnification should allow you to see the darkfield stop in the brightfield image.

7. Using condenser lens centering screws, move the darkfield stop to the center of the image.
8. Once centered, slowly lower the condenser until the background is as dark as possible and the darkfield stop is a dark disk. Raise the condenser back up and the dark disk should appear bright (Fig. 2).
9. Switch to the 100x adjustable iris objective.
10. With the iris closed ~ 2/3 of the way focus on the cheek sample again. (Fig. 3a)
11. Now switch to a sample of stabilized microtubule seeds. (Fig. 3b) (see Note 6).
12. Adjust the light intensity, iris size, and exposure time to suit your experiment (see Note 7)

3.2. Making double-cycled GMPCPP-stabilized biotinylated microtubule seeds

1. Mix 5 μL of 2 mg/mL biotin-tubulin with 95 μL of 2 mg/mL unlabeled tubulin and incubate on ice for 5 min. This results in microtubules that have ~5% of tubulin biotin labeled.
2. Spin the tubulin mixture to remove any tubulin aggregates at 279,000Xg in an ultracentrifuge using a TLA-100 rotor (Beckman) for 10 minutes at 4°C. Make sure to pre-chill your tubes.
3. Add GMPCPP to a final concentration of 0.5mM and incubate at 37°C for 1h.

   Spin the microtubules in an ultracentrifuge at 126,000Xg for 15 minutes at 37°C.
4. Remove the supernatant. Gently wash the pellet with warm BRB80.
5. Resuspend the tubulin pellet in cold BRB80 such that the final tubulin concentration is ~ 2mg/ml (see Note 8).
6. Incubate on ice for 30 minutes, mix by pipetting gently every 10 minutes.
7. Add GMPCPP to a final concentration of 0.5mM and incubate in 37°C water bath (or heat block) for 30 minutes.
8. Spin microtubules at 126,000Xg for 15 minutes at 37°C in a TLA100 ultracentrifuge rotor.
9. Remove the supernatant without touching the pellet. Gently wash the pellet with warm BRB80.
10. Gently resuspend the microtubule seeds in warm BRB80 (see Note 9).
11. Flash-freeze in small aliquots. On the day of performing the assays, dilute a seed aliquot 1:10 in warm BB and place at 37°C for 1h before use.

3.3 Flow-Chamber Assembly

1. Place two pieces of double-sided tape on a silanized microscope slide such that they are parallel and 3–4mm apart.

2. Using a sharp blade trim the excess tape off the edge of the slide.
3. Place a silanized coverslip on the tape such that its long axis is perpendicular to the long axis of the microscope slide.
4. Using gentle pressure press down on the slide to ensure it is sealed to the double-sided tape.

3.4 Chamber Preparation and Image Acquisition

1. On the day of performing the assay, filter all solutions through a 0.1 μm filter by spinning at 10,000xg for 2 minutes (see Note 10).
2. Turn on all equipment and start heating the microscope objective. (see Note 11).
3. Thaw seeds, dilute 1:10 in warm BB and place at 37°C for at least one hour (see Note 12).
4. Thaw tubulin on ice and ultracentrifuge for 10 minutes at 276,000 x *g* at 4°C in a TLA100 ultracentrifuge rotor (see Note 13).
5. Perfuse the chamber with 20–40 μl of room temperature BRB80 (see Note 14).
6. Perfuse the chamber with 20 μl of ice cold Neutravidin solution and wait 5–10 minutes.
7. While the neutravidin incubates, remove your tubulin from the centrifuge and check the concentration by Bradford assay.
8. Wash the chamber with 2x chamber volumes (~20 μl) of BBC and 2x chamber volume (~20 μl) of BBP. (see Note 15).
9. Perfuse in 20 μl of seeds at an appropriate dilution. Wait 5–10 minutes. (see Note 16).
10. Check the density of seeds by imaging the chamber. If there are too many seeds, or if the chamber looks dirty, start over and prepare a new one. Save an image of the seeds in the area of interest. This can be used to demarcate where the seeds end and the dynamic microtubule extension begins. Alternatively, seeds can be prepared with fluorescent tubulin and imaged first using fluorescence microscopy.
11. Wash the chamber with 2x chamber volumes (~20 μl) of BBC and 2x chamber volume (~20 μl) of BBP.
12. Perfuse in Dynamics buffer (20 μl perfusion volume). (see Note 17)
13. Seal the chamber with vacuum grease to prevent evaporation.
14. Find a suitable area and image microtubules for 30 minutes. We image at a frame rate of 2 Hz for quantifying growth rates, catastrophe and rescue frequencies, and a rate of 20–40 Hz for quantifying depolymerization rates.

3.5 Data analysis

Microtubule dynamic parameters are measured by tracing the microtubule tip positions over time and generating kymographs. The slope represents the growth rate. Catastrophes mark the switch from growth to depolymerization. Rescues mark the switch from depolymerization to growth (Fig. 4). To obtain reliable kymographs, movies should first be corrected for drift. This entire process can be performed in many software packages. We use ImageJ/FIJI.

1. To correct for drift, a registration Plugin in FIJI can be used (28). (see Note 18)
2. Scroll through the drift corrected movie to generate kymographs of each microtubule (Fig. 4). From kymographs extract the polymerization and depolymerization rates, catastrophe frequency (number of catastrophe per time microtubule spent growing) and rescue frequency (number of rescues per time spent depolymerizing). As an alternative to analyzing kymographs manually there are now several automated solutions available. They will either analyze the kymograph directly (29) or track the growing tips of microtubules and extract dynamic parameters form tip positions. (30, 31)

4. Conclusions

This chapter describes a protocol for imaging *in vitro* microtubule dynamics using darkfield microscopy. Darkfield imaging is easy and cheap to integrate into an existing inverted microscope. The label free nature of the technique allows one to image with high signal-to-background ratios, at high frame rates and without photobleaching, an unavoidable downside of fluorescence-based imaging. In conclusion, darkfield microscopy, and label-free imaging techniques in general, allow the study of tubulin isoforms that are in low abundance and not amenable to fluorescent labeling. These techniques are making a comeback in the microtubule field, catalyzed by the recent exciting advances in expressing and purifying single-isoform tubulin and isolating tubulin from diverse sources using affinity approaches.

5. Notes

1. A high NA oil immersion condenser is necessary in order to obtain high quality images. There are many different commercially available options. Our lab uses a Nikon Darkfield Oil Immersion NA 1.4 condenser, but several other manufactures make darkfield condensers as well. Imaging microtubules requires a well aligned condenser and the appropriate iris size on the objective. The NA of the condenser needs to be higher than the NA of the objective to achieve darkfield imaging. We use a 1.45 NA condenser and a 1–1.3 NA adjustable 100x objective from Nikon but there are other commercial options available (i.e. Leica, Zeiss, Olympus).
2. Prepare the Neutravidin stock solution at 1mg/mL as *per* manufacturer's protocol. Flash freeze and store at −80°C in small aliquots.
3. After thawing on ice, the tubulin needs to be ultracentrifuged at 230,000Xg for 10 minutes at 4°C to remove any tubulin aggregates. Make sure to pre-chill the

ultracentrifuge tubes as well as the rotor. Measure tubulin concentration after the spin by Bradford or A280 absorbance.

4. Add tubulin to the perfusion mixture last. Make sure there are no bubbles as tubulin and proteins in general denature at the air-liquid interface. Mix and use immediately.

5. Light exits above the critical angle when using a high NA darkfield condenser, therefore no light will exit the condenser until the slide makes contact with the oil. As the condenser approaches the sample and makes contact with the oil a flash of light is observed. This is an indication that the condenser has made oil contact with the top side of your chamber. The condenser that we use has a working distance that is slightly larger than the thickness of the slide (~ 1mm), therefore we are imaging microtubules attached to the slide surface (in contrast to interference techniques which image microtubules that are growing from seeds immobilized to the coverslip). Because of this, the correct focal plane may be slightly higher for darkfield than for TIRF imaging.

6. You will only be able to image the stabilized microtubules if the cheek cell slide was properly aligned. First, check that the condenser spot is still centered on the field of view of your camera. Next, adjust all apertures to allow the maximum amount of light possible to enter the sample. Adjust the objective iris until the background is a light grey. If necessary, make small adjustments to the position of the condenser. When at the proper focal plane, the microtubules will appear bright on a dark background. It may also be necessary to adjust the size of the illumination using the field stop. Note that you might need to adjust the image histogram to obtain a good image. Software autoscaling will make it difficult to observe the microtubules if there are very bright objects near them.

7. There is a tradeoff between signal-to-noise, imaging speed and the size of the objective iris. We find that closing the iris ~2/3 of the way gives good signal for exposure times as low as 20 ms. If high speeds are not necessary, one can also adjust the brightness of the light source and use longer exposure times (~ 200 ms).

8. For brain tubulin, the typical polymerization efficiency is ~70%. Therefore, resuspend the pellet with a volume such that the concentration will be 2mg/ml.

9. Cut the pipet tip to prevent shearing when pipetting the microtubule seeds.

10. Any scattering mass in the sample will obscure your darkfield signal. We find filtering our solutions through a 0.1μm filter allows us to obtain high quality darkfield images. Moreover, we would like to emphasize that the sample has to be very clean and free of aggregates. This is one of the challenges of darkfield microscopy. Unlike fluorescence microscopy where one sees only what is labeled, any scattering mass will give a signal in darkfield microscopy. It is not uncommon for a sample to look “clean” with high signal-to-background in TIRFM, but have extremely high background in darkfield because of the

scattering from a very small amount of aggregates. Thus, high sample quality is paramount.

11. We use a Bioptechs objective heater but there are many commercial objective heaters available.

12. After incubating the seeds at 37°C, store them at room temperature. This incubation time gives an average seed length of 1–3 μm. If longer seeds are desired incubate at 37°C for a longer time.

13. Tubulin can be stored on ice for ~ 1–1.5h but should not be stored longer as it tends to aggregate on ice over time and this will compromise polymerization behavior.

14. If your glass is silanized and cleaned well, the initial perfusion may prove to be difficult. One can either pipette the solution a few times and try not to introduce bubbles, or use a vacuum line to draw the liquid through.

15. In our experience having casein in the chamber during imaging tends to compromise image quality.

16. We often check the seed dilution before proceeding to make sure there are a good number of seeds in the field of view and the chamber is not sparse or crowded. It is a good idea to prepare a few chambers at different seed dilutions to determine the correct density before starting assays for the day.

17. Do not perfuse ice-cold solutions into the chamber as that will depolymerize the seeds! You can hold the perfusion in your hand for 1–3 seconds to warm it up.

18. Drift correction can be done using spots on the glass as fiducial markers. We almost always have a few bright spots on the glass that we are able to use as landmarks for registration. Fiducial beads can also be immobilized in the chamber with the seeds if needed, but we have not found this to be necessary.

References

1. Kuriyama R, Miki-Noumura T (1975) Light-microscopic observations of individual microtubules reconstituted from brain tubulin. Journal of cell science 19:607–620 [PubMed: 173726]
2. Mitchison T, Kirschner M (1984) Dynamic instability of microtubule growth. nature 312:237 [PubMed: 6504138]
3. Walker RA, O'brien ET, Pryer NK et al. (1988) Dynamic instability of individual microtubules analyzed by video light microscopy: rate constants and transition frequencies. J Cell Biol 107:1437–1448 [PubMed: 3170635]
4. Horio T, Hotani H (1986) Visualization of the dynamic instability of individual microtubules by dark-field microscopy. Nature 321:605 [PubMed: 3713844]
5. Summers K, Kirschner MW (1979) Characteristics of the polar assembly and disassembly of microtubules observed in vitro by darkfield light microscopy. The Journal of cell biology 83:205–217 [PubMed: 511939]
6. Akhmanova A, Steinmetz MO (2015) Control of microtubule organization and dynamics: two ends in the limelight. Nat Rev Mol Cell Biol 16:711–726 [PubMed: 26562752]
7. Guo H, Xu C, Liu C et al. (2006) Mechanism and dynamics of breakage of fluorescent microtubules. Biophysical journal 90:2093–2098 [PubMed: 16387782]

8. Aumeier C, Schaedel L, Gaillard J et al. (2016) Self-repair promotes microtubule rescue. Nat Cell Biol 18:1054–1064 [PubMed: 27617929]
9. Vigers GP, Coue M, Mcintosh JR (1988) Fluorescent microtubules break up under illumination. J Cell Biol 107:1011–1024 [PubMed: 3417772]
10. Widlund PO, Podolski M, Reber S et al. (2012) One-step purification of assembly-competent tubulin from diverse eukaryotic sources. Mol Biol Cell 23:4393–4401 [PubMed: 22993214]
11. Vemu A, Garnham CP, Lee DY et al. (2014) Generation of differentially modified microtubules using in vitro enzymatic approaches. Methods Enzymol 540:149–166 [PubMed: 24630106]
12. Vemu A, Atherton J, Spector JO et al. (2016) Structure and Dynamics of Single-isoform Recombinant Neuronal Human Tubulin. J Biol Chem 291:12907–12915 [PubMed: 27129203]
13. Minoura I, Hachikubo Y, Yamakita Y et al. (2013) Overexpression, purification, and functional analysis of recombinant human tubulin dimer. FEBS Lett 587:3450–3455 [PubMed: 24021646]
14. Ti SC, Pamula MC, Howes SC et al. (2016) Mutations in Human Tubulin Proximal to the Kinesin-Binding Site Alter Dynamic Instability at Microtubule Plus- and Minus-Ends. Dev Cell 37:72–84 [PubMed: 27046833]
15. Johnson V, Ayaz P, Huddleston P et al. (2011) Design, overexpression, and purification of polymerization-blocked yeast alphabeta-tubulin mutants. Biochemistry 50:8636–8644 [PubMed: 21888381]
16. Chaaban S, Jariwala S, Hsu CT et al. (2018) The Structure and Dynamics of C. elegans Tubulin Reveals the Mechanistic Basis of Microtubule Growth. Dev Cell 47:191–204 e198 [PubMed: 30245157]
17. Weisenberg RC (1972) Microtubule formation in vitro in solutions containing low calcium concentrations. Science 177:1104–1105 [PubMed: 4626639]
18. Vemu A, Atherton J, Spector JO et al. (2016) Structure and dynamics of single-isoform recombinant neuronal human tubulin. Journal of Biological Chemistry 291:12907–12915 [PubMed: 27129203]
19. Geyer EA, Burns A, Lalonde BA et al. (2015) A mutation uncouples the tubulin conformational and GTPase cycles, revealing allosteric control of microtubule dynamics. Elife 4:e10113 [PubMed: 26439009]
20. Andrecka J, Arroyo JO, Lewis K et al. (2016) Label-free imaging of microtubules with sub-nm precision using interferometric scattering microscopy. Biophysical journal 110:214–217 [PubMed: 26745424]
21. Mahamdeh M, Simmert S, Luchniak A et al. (2018) Label-free high-speed wide-field imaging of single microtubules using interference reflection microscopy. Journal of microscopy 272:60–66 [PubMed: 30044498]
22. Simmert S, Abdosamadi MK, Hermsdorf G et al. (2018) LED-based interference-reflection microscopy combined with optical tweezers for quantitative three-dimensional microtubule imaging. Optics express 26:14499–14513 [PubMed: 29877486]
23. Katsuki M, Drummond DR, Osei M et al. (2009) Mal3 masks catastrophe events in Schizosaccharomyces pombe microtubules by inhibiting shrinkage and promoting rescue. J Biol Chem 284:29246–29250 [PubMed: 19740752]
24. Kandel ME, Teng KW, Selvin PR et al. (2017) Label-Free Imaging of Single Microtubule Dynamics Using Spatial Light Interference Microscopy. ACS Nano 11:647–655 [PubMed: 27997798]
25. Ueno H, Nishikawa S, Iino R et al. (2010) Simple dark-field microscopy with nanometer spatial precision and microsecond temporal resolution. Biophys J 98:2014–2023 [PubMed: 20441766]
26. Edelstein AD, Tsuchida MA, Amodaj N et al. (2014) Advanced methods of microscope control using muManager software. J Biol Methods 1
27. Ziółkowska NE, Roll-Mecak A (2013) In vitro microtubule severing assays. Methods Mol Biol 1046:323–334 [PubMed: 23868597]
28. Schindelin J, Arganda-Carreras I, Frise E et al. (2012) Fiji: an open-source platform for biological-image analysis. Nat Methods 9:676–682 [PubMed: 22743772]
29. Mukherjee A, Jenkins B, Fang C et al. (2011) Automated kymograph analysis for profiling axonal transport of secretory granules. Med Image Anal 15:354–367 [PubMed: 21330183]

30. Kapoor V, Hirst WG, Hentschel C et al. (2019) MTrack: Automated Detection, Tracking, and Analysis of Dynamic Microtubules. Sci Rep 9:3794 [PubMed: 30846705]

31. Ruhnow F, Zwicker D, Diez S (2011) Tracking single particles and elongated filaments with nanometer precision. Biophys J 100:2820–2828 [PubMed: 21641328]

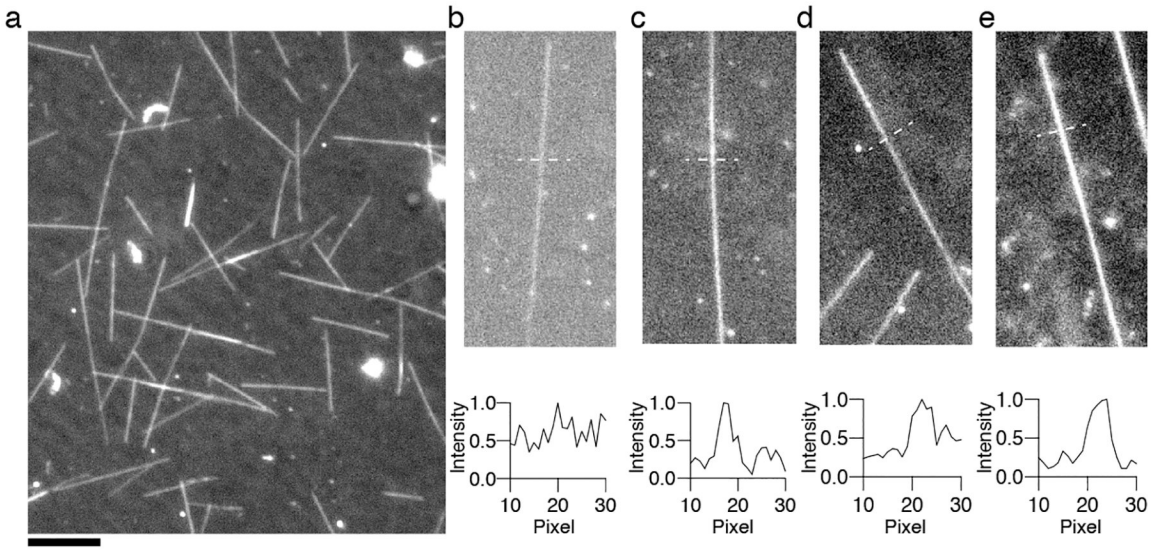

Figure 1.

Darkfield image of growing microtubules imaged at 20 Hz. Scale bar represents 10 μm. (a). Images of a single microtubule and normalized line scans across the dotted white line at 10, 25, 50 and 100 ms exposure times respectively (b-e).

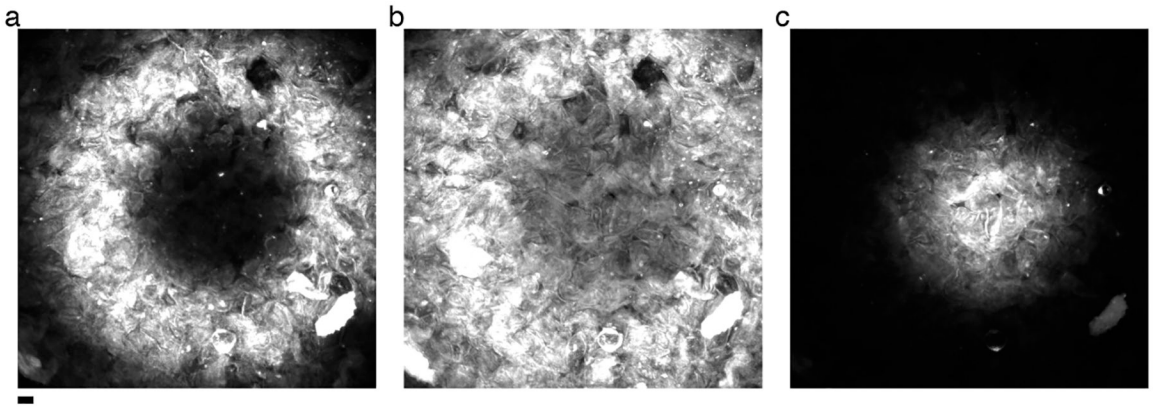

Figure 2.

Examples of low magnification images of cheek cells. The darkfield stop will appear initially as a dark disk (a). As the condenser moves down, the central spot will get brighter (b). When the correct position is reached, the cells look bright while the background remains dark (c). At this point good alignment is achieved and you can switch to higher magnification. Scale bar represents 50 μm.

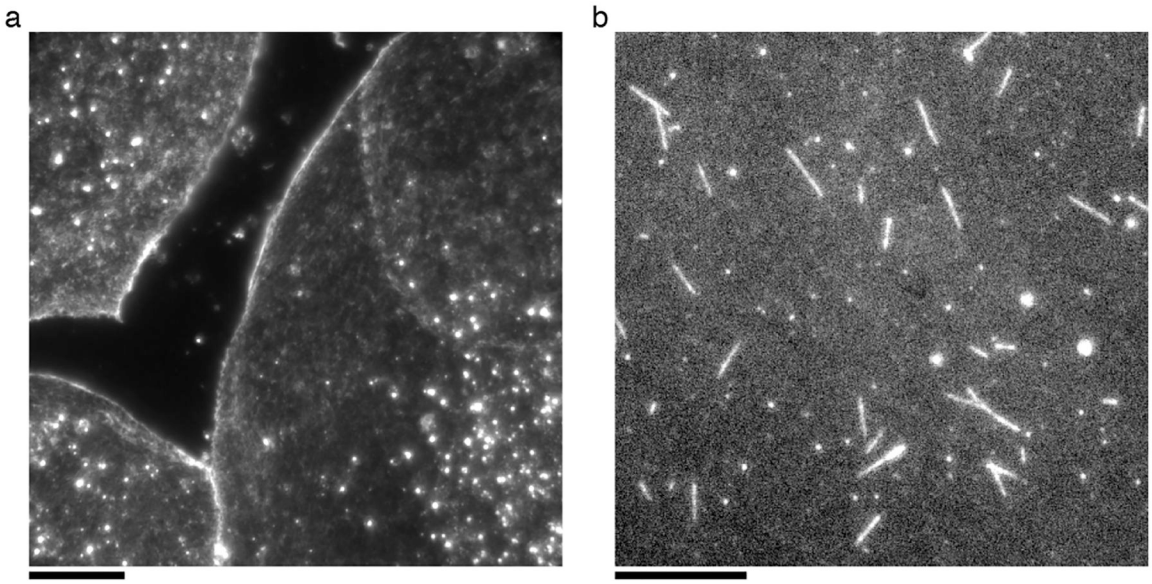

Figure 3.

Images of well-aligned cheek cells at 100x magnification. Scale bar represents 20 μm (a). Images of immobilized microtubule seeds. Scale bar represents 10 μm.(b)

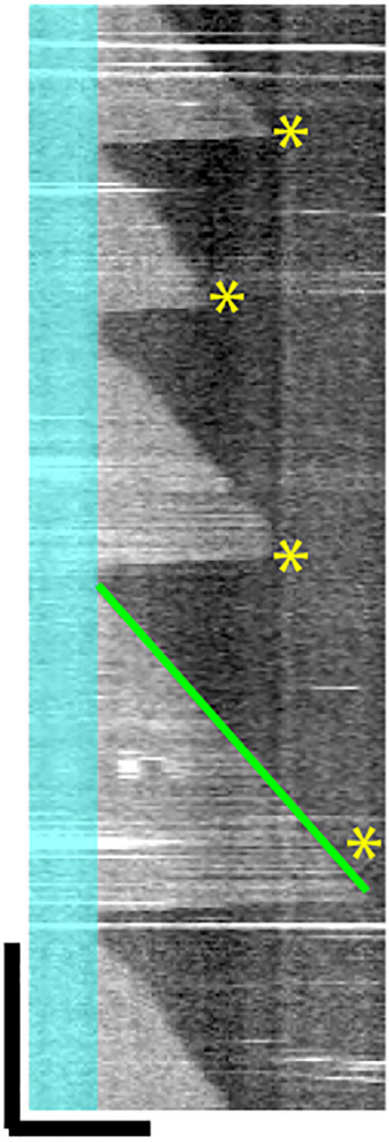

Figure 4.

A kymograph of a representative microtubule imaged in darkfield. The bright streaks represent scattering objects that were rapidly diffusing in solution. The stabilized seed has been pseudo-colored in blue. Yellow stars represent a catastrophe event. The slope of the green line is used to calculate the growth rate. Scale bar represents 5 μm horizontally and 5 min vertically.